Structural, thermal, and mechanical properties of gelatin-based films integrated with tara gum

Structural, Thermal, and Mechanical properties of gelatin-based films integrated with tara gum

Luca Nuvoli,[a] Paola Conte,[b] Costantino Fadda, [b] José Antonio Reglero Ruiz,[c] José Miguel García Pérez,[c] Salvatore Baldino[d] and Alberto Mannu[d]*

[a] Department of Chemistry and Pharmacy, University of Sassari and INSTM, Via Vienna 2, 07100 Sassari, Italy.

[b] Department of Agriculture, University of Sassari, Viale Italia 39/A, 07100 Sassari, Italy.

[c] Departamento de Química, Facultad de Ciencias, Universidad de Burgos, Plaza de Misael Bañuelos s/n, 09001 Burgos, Spain.

[d] Dipartimento di Chimica, Università di Torino, Via Pietro Giuria, 7, I-10125 Torino, Italy.

*Corresponding author e-mail: alberto.mannu@unito.it

Abstract

Films with different morphology can be obtained by mixing fish gelatin, Tara gum and glycerol in different ratio and by subjecting the Tara gum to a ball milling treatment before its use. The amount of the plasticizer glycerol, as well as the type of Tara gum employed (as received or milled) resulted, from SEM and AFM analyses, to strong influencing the morphology of the films and their density. Also, the morphological differences determine different thermal and mechanical behaviours. In particular, the employment of milled Tara gum allows to improve the thermal stability, as well as the mechanical properties of the polymers. A similar outcome can be obtained by increasing the glycerol content, which can be used up to 20 wt%. Glycerol amounts exceeding that percentage, are detrimental for the quality of the films and reduce their thermal and mechanical performances.

Keywords: Tara gum; gelatin fish; biofilms

1. Introduction

During the last years, fervent research activities have been conducted on the engineering of composite gels. The possibility to tune gel properties combining specific components has gained increasing importance in many application fields, including food, drug delivery, tissue engineering and wound dressing [1,2,3].

Among the several components usually employed for composite gels engineering, gelatin, a mix of denaturated proteins derived by collagen [4,5,6], have attracted particular interest for biomedical and food packaging sectors, due its remarkable properties. As a matter of fact, gelatin is biocompatible, biodegradable, shows high capacity of cell adhesion and migration [7], shows antimicrobial properties [8], and it has been successfully exploited for tissue engineering [9,10]. Thermal properties of gelatin have been characterized in different papers. For example, Rahman *et al.* [11] presented a complete study about the glass transition and melting points of commercial mammalian gelatin, tuna gelatin, bovine gelatin and porcine gelatin. Glass transitions temperatures varied from 23 to 75 ºC, whereas melting points were measured between 115 and 190 ºC. These wide range of values, combined to their biocompatibility, make them suitable in many different biomedical applications, such as drug delivery or tissue engineering [12,13]. Of particular interest, especially for the packaging and biomedical sectors, are the Fish Gelatin (FG) based films. FG is cheap, biodegradable and easy to process for making films. In addition, its mechanical and optical properties can be modulated by adding polyols which act as plasticizers. The main role of

such additives consists in the denaturation of the FG's proteins by reducing the interactions between protein chains and modifying the secondary, tertiary and quaternary structures [14]. Within the polyols commonly employed for such purpose, glycerol stands out as the ideal candidate. It showed good ability to interact with FG, eco-compatibility, and it is available in large amount as by-product of waste vegetable oils treatment [15], e.g. from biodiesel production [16]. On the other hand, the use of fish gelatin in composite films is still limited by several factors such as low stability, poor mechanical strength and low elasticity [17]. Many studies have been then conducted with the aim to solve these weaknesses by exploring the doping with different additives including synthetic and biological polymers [18]. Although different studies have been performed on the use of FG in composites in combination with various additives, the interaction between gelatin and different natural gums in modifying the thermal and mechanical properties of gelatin has been only recently explored [19]. Natural gums have shown to allow structural engineering of thin films while guaranteeing the biodegradability and edibility of the material [20]. Specific combinations between natural gelatin, glycerol and natural gums have found important application especially in food packaging [18].

Regarding the most employed natural gums (Tara, guar, and locust beam), Tara gum (Ta) shows intermediate water solubility with respect to guar (cold soluble) and locust beam gum (cold insoluble), making it ideal e.g. as food hydrocolloid [20]. Tara gum is obtained by grinding the endosperm of the seeds of Caesalpinia spinosa (Fam. Leguminosae) and it is composed by polysaccharide chains of high molecular weight based on the galactomannan unit (See **Scheme S1** of the Electronic Supplementary Information file, **ESI**). It has been approved as food additive due to its non-toxicity and thus it has gained value as film additive [21]. When employed in gel composites, tara gum acts as thickening agent and stabilizer.

In this context, herein, the fabrication and characterization of novel films based on fish gelatin (FG), Tara gum (Ta), and glycerol (Gly), is reported. Ten films containing different ratio of FG/Ta, different glycerol content and different types of Ta, are described and characterized. For each film the structural, thermal, and mechanical properties are discussed by meaning of, respectively, IR, X-ray, and SEM, Thermogravimetry (TG) and differential scanning Calorimetry (DSC), and tensile properties analyses.

2. Materials

Tara gum (Aglumix 01, particle size 149 μm) and Fish Gelatin (LapiFish, particle size 2380 μm) were purchased, respectively, from Silvateam Food Ingredients S.r.l. and Lapi gelatin

S.p.a.. Fish gelatin with the following characteristics was employed: Bloom 280, mesh size 8-70, protein amount between 85% and 90%, water content 10-12%, and salts content 1-2% [22].

Glycerol (90%) was purchased from Analyticals Carlo Erba, while acetone (>99%) and ethanol (>99.5%) from VWR. All chemicals were used as received without any further purification.

3. Experimental equipment and methods

Fourier transform infrared (FTIR) analysis was performed using a Bruker infrared Vertex 70 interferometer. The spectra were recorded on the films in transmission mode, in the 400-4000 cm^{-1} range by averaging 64 scans with 4 cm^{-1} of resolution.

Principal Component Analysis (PCA) as well as Partial Least Squares Discriminant Analysis (PLS-DA) were conducted using of the tool Metaboanalyst 4 [23]. The spectral data were centered and auto-scaled before the PCA and PLS-DA analysis.

The XRD patterns were collected using a Rigaku SmartLab X-ray powder diffractometer aligned according to a Bragg–Brentano geometry with Cu Kα radiation (λ = 1.54178 Å) and equipped with a graphite monochromator in the diffracted beam. Since the polymers showed broad haloes typical of amorphous condition, it was deliberately assumed to restrict the reciprocal space investigation in the angular range from 5° to 80° in 2θ, which allows to determine the main shape features of specimen. Powders have been deposited in an amorphous glass sample holder for measurements.

Ball milling of the Ta powders (15 g) was carried out in a SPEX Mixer/Mill 8000 at a rotation speed of 875 rpm during 1 h, using two zirconia balls of 2 g each one. Taking in consideration the very low amount of powders which are usually trapped (1 mg) at each impact, and the stochastic nature of the ball milling process, over 200k collisions, occurring under the mechanochemical conditions above reported, should be enough for refining homogenously all the batch powders [24]. Then, two different Tara gum powders were obtained: as received (or non-milled) and milled.

The morphologies of the powders and films were observed by different techniques. First, SEM images were taken using a FEI Quanta 200 scanning electron microscope. The samples were placed on a double-sided carbon tape and examined at an acceleration voltage of 20 kV under high vacuum. Also, Atomic Force Microscopy (AFM) images were taken at RT using a confocal AFM-RAMAN model Alpha300R – Alpha300A from WITec, using an AFM tip of 42 N/m.

The thermogravimetric analysis data were recorded on a TA Instrument Q50 TGA analyzer. TGA tests were performed under O_2 (synthetic air) atmosphere using the next procedure: first, samples were heated from RT to 100 °C at 10 °C/min, and then kept during 10 min to eliminate the moisture content. Then, samples were heated up to 800 ºC at 10 ºC/min.

DSC analyses were performed using a DSC Q200 TA Instruments equipment. Samples were tested using a four-cycle procedure [25]. In the first cycle, after 5 min of stabilization at RT, samples were heated up to 150 °C at 10 °C/min and then stabilized during 5 min before cooling down in the second cycle to 30 °C at 20 °C/min. In the third cycle, samples were heated up to 150 °C at 10 °C/min and after 5 min of stabilization at 150 °C, the fourth cycle was performed: samples were cooled down to 30 °C at 20 °C/min. All the tests were performed under N_2 atmosphere (flow rate 50 ml/min). Mass of the samples was fixed at approximately 20 mg in each test. Glass transition temperature (T_g) was determined in the third cycle.

To determine the tensile properties of the films, strips of 5 mm in width and 35 mm in length were cut from each film. Tensile tests were carried out on a SHIMADZU EZ Test Compact Table-Top Universal Tester at 20 °C. Mechanical clamps were used and an extension rate of 5 mm/min was applied using a gauge length of 9.44 mm. At least 4 strips were tested for each film in order to calculate the average value for each parameter determined.

4. Preparation of films

The preparation of gelatin-based films is here detailed and schematized in **Figure S1** of the **ESI**. Tara powder was added to a solution of glycerol and distilled water and the mixture was stirred at 85°C during 30 minutes until a homogeneity was reached (**I**). Then, Fish gelatin was added at 85 °C and stirred until dissolution (**II**). The mixture was subjected to ultrasound for 15 minutes to remove air bubbles (**III**). Film-forming solutions were poured into Steriplan® petri dished (80 mm x 15 mm) and dried at room temperature for 6 h and then located at 50 °C in humidity-controlled oven for 16 hours (**IV**). The corresponding film was thoroughly washed with ethanol and acetone to afford the desired gel.

5. Results and discussion

5.1 Density and visual aspect of the films

Ten films composed by Fish gelatin (FG), Tara powder (Ta) and glycerol (Gly) were prepared with different Ta/FG ratio (1/2, 1/1, and 2/1) and Gly amount (20, 40, and 60 wt%). Additionally, two reference films (FG/Gly and Ta/Gly) were also prepared to compare their

properties with the FG/Ta/Gly films. Finally, two types of Ta were considered: as received by the purchaser, and milled. Nomenclature, density and composition of the films fabricated are reported in **Table 1**.

Table 1. Nomenclature, density and composition of the films fabricated.

Film	FG (eq. wt.)	Ta (eq. wt.)	Ball Milling	Gly (wt%)	Density (g/cm^3)
TGG01	1	1	No	20	7.9
TGG02	1	1	Yes	20	8.6
TGG03	1	1	No	40	6.8
TGG04	1	1	Yes	40	8.2
TGG05	1	1	No	60	6.5
TGG06	1	1	Yes	60	7.2
TGG07	2	1	No	20	7.8
TGG08	2	1	Yes	20	8.7
TGG09	1	2	No	20	9.1
TGG10	1	2	Yes	20	9.8
FG/Gly	1	0	No	20	4.7
Ta/Gly	0	1	No	20	10.0

Table 1 shows that densities obtained vary from 6.5 g/cm^3 for TGG05 film to 9.8 g/cm^3 for TGG10 film. Also, it can be noticed that the density of the as-casted films increases for systems containing milled Tara powder compared to those produced using the non-milled one (TGG02 vs TGG01). A relevant influence glycerol content on the density values was observed, which decrease at higher wt% of glycerol (TGG06 vs TGG02). As expected, pure FG film shows the lower density value (4.7 g/cm^3), while pure Tara film presents the higher density value (10.0 g/cm^3).

From a qualitative visual analysis, film specimens were transparent despite Ta/Gly presented a slightly yellow to brown appearance with respect to FG/Gly film. On the other hand, in TGG01 to TGG10 films opaqueness is reduced. This means that opacity could be related to the Tara adding effect and its dispersion during film preparation, causing the reduction of the film transparency with respect to starting Fish gelatin film. This characteristic could limit the use of films composed by only Tara in food packaging applications. In **Figure 1** the photographs of the films FG/Gly, Ta/Gly, TGG01 and TGG02 are shown.

Figure 1. Photographs of the FG/Gly, Ta/Gly, TGG01 and TGG02 films.

5.2 FT-IR analysis

A first quality check on the effect of the preparation procedure on the chemical composition of the constituents of films TGG01-TGG10 was performed by FTIR analysis. Results are displayed in **Figure S2** of the **ESI**. The absorption bands for gelatin-based composite films in the IR spectra are situated in the amide band region. The band situated around 3299, 1635, 1550, 1238 cm^{-1} correspond to amide-A (NH-stretching coupled with hydrogen bonding) and water molecules, amide I (C=O stretching/hydrogen bonding coupled with COO), amide II (bending vibration of N–H groups and stretching vibrations of C–N groups), and amide III (vibrations in the plane of C–N and N–H groups of bound amid). The bands in the FTIR spectrum of Tara powder appear in two major regions, 3700-2500 cm^{-1} and 1700-700 cm^{-1}. The broad band at 3700-3000 cm^{-1} is a result of O-H stretching vibration which is associated with free, inter and intra-molecular bonded hydroxyl groups. The shoulder-shaped band at about 2920 cm^{-1} is the stretching vibration of $-CH_2$. The bands at 1020 cm^{-1} is characteristic of the O-C stretching vibration of the anhydro glucose ring. These bands indicate that Tara powder has the general properties of a polysaccharide [26,**Error! Bookmark not defined.**].

If from one side the FT-IR data confirm the expected composition of the films, ruling out any thermal decomposition which can occur during the synthesis from the other side, [27,**Error! Bookmark not defined.**] by a visual analysis of the plots reported in **Figure S2**, few information can be obtained on the differences between films with different composition [28,29].

In order to analyse better the available FT-IR data and to extrapolate as more information as possible, a multivariate analysis of the spectral data was conducted. The normalized frequencies relative to films TGG01-TGG10 were considered for building a spectral fingerprint of each film. The aim of such statistical analysis was to distinguish between films

containing milled and not-milled Tara. At first, non-supervised Principal Component Analysis (PCA) was conducted, as shown in **Figure S3** of the **ESI**.

As expected, PCA analysis of the FT-IR intensities doesn't allow to reach a perfect discrimination. In fact, unbiased PCA method works properly when within-group variation, [30] in this case related with FG/Ta ratio and glycerol content, is sufficiently less than between-group variation (milled and not-milled Tara). Nevertheless, a supervised approach as the Partial Least Squares Discriminant Analysis (PLS-DA) can be used for classify the two considered groups and discuss properly differences between films, as it is presented in **Figure S4** of the **ESI**, in which 2D Component 1 vs Component 2 Plot of FT-IR intensities of films TGG01-TGG10, containing milled (M) and not-milled (NM) Ta are shown.

From the information of **Figure S4** it is possible to appreciate the discrimination between films contained milled and not-milled Ta obtained through multivariate PLS-DA analysis. The analysis, even qualitative, of the distances between the labels in the Scores Plot is of particular interest. Comparing films containing milled (M) and not-milled (NM) Tara, it is possible to notice incremental differences following the trend TGG03-TGG04, TGG05-TGG06, TGG07-TGG08, and TGG09-TGG10, indicating an increasing effect of the Ta grain size which depend on the amount of glycerol and on the FG/Ta ratio. More glycerol is present, more the milled Tara is distinguishable from the not-milled one (TGG02, TGG04, TGG06 vs TGG03, TGG05, and TGG07). As matter of fact, films containing an FG/Ta ratio of 1/2 or 2/1 seems to be more sensitive to the type of Tara (TGG08, TGG10 vs TGG09, and TGG10). FT-IR qualitative analysis highlighted important chemical differences within films with different glycerol content and Tara typology. If the effect of the plasticizer (glycerol) it is known and expected, the possibility to affect the composition of a film by changing the granulometry of the Tara deserves more attention.

5.3 X-ray diffraction analysis

With the aim to better assess the structural differences between films TGG01-TGG10, X-ray diffraction analysis was conducted. Figure **S5** of the **ESI** displays the XRD patterns of all the films prepared. Ta presents a broad peak at ~19° indicating amorphous and crystalline regions existed because a large amount of –OH groups interacted via intermolecular hydrogen bonds. This peak partially disappeared in the composite film, indicating that a part of Tara molecules was in ordered arrangement, which was interrupted in the grafting process; therefore, the obtained composite is amorphous. After grafting, the

peak strength decreased, which indicated that intermolecular hydrogen bonds were damaged.

The diffractogram pattern acquired on the FG/Gly film was typical of a partially crystalline gelatin with a sharp peak located at 2θ = 7.1° (d_{101} = 12.29 Å) and a broad peak located at 2θ = 20° (d_{101} = 4.0 9 Å), as shown in **Figure S5**. These characteristic peaks are usually assigned to the triple-helical crystalline structure in gelatin. In particular, the first diffraction peak at 7° (sharp and intense) is directly related to the diameter of the triple helix. It was also found that the addition of polyols such as glycerol most often decreases the intensity of the first peak (2θ = 7°). Furthermore, it has been observed that the addition of tara gum shifted the diffraction angle from 7.1° to 9.12° (for TGG05/06 and TGG09/10 films) then decreasing the diameter of the inter reticular triple helix. On the other hand, this intensity of peaks decreases and, in some cases, completely disappeared (TGG01/02, TGG03/04 and TGG07/08 films). The disappearance of X-ray diffraction peaks corresponding to the composites films confirms the interaction between two biopolymers. This phenomenon illustrates the reduction hydrogen bonds between hydroxyls group of gelatin and those of anhydroglucose of Tara gum, which limited the movement of molecules and thus prevented crystallization.

The addition of glycerol seems to decrease the intensities of the gelatin peak making the film more amorphous as compared to control gelatin film. This is probably due to the high stability of these films when glycerol was added. Finally, a clear effect of BM was observed only on TGG06 system which presented a significant decrease on the peak intensity at 2θ =19.9° with respect to TGG05. This effect could be related with the synergic effect of glycerol addition and Tara gum added with refined particle size, and it confirms the influence of Tara granulometry qualitatively observed by FT-IR.

5.4 Morphological analysis

An exhaustive morphology analysis of the films TGG01-TGG10 was conducted by different approaches. Firstly, Scanning Electron Microscopy (SEM) images of the films were collected as shown in **Figure 2**.

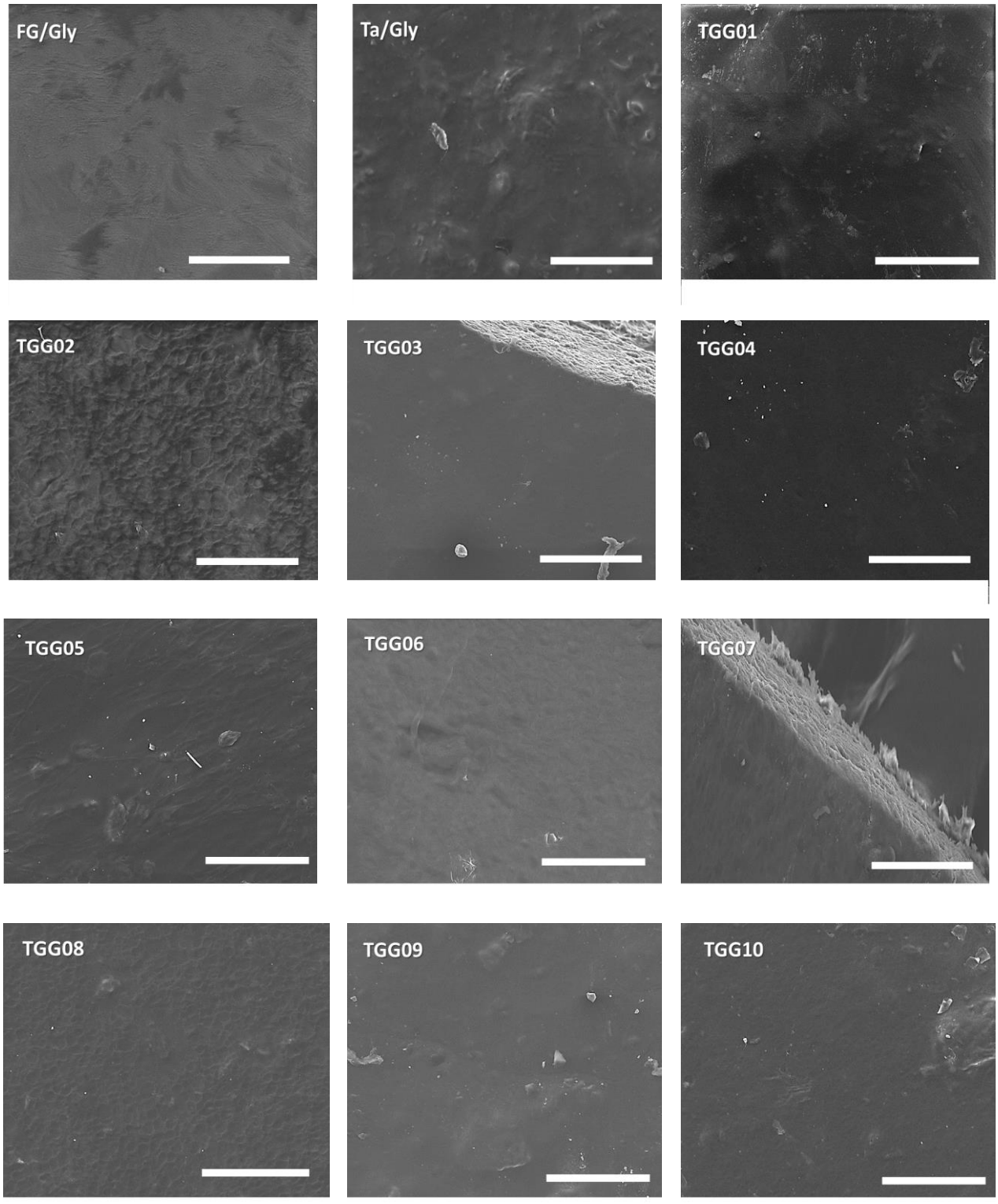

Figure 2. SEM images of the films prepared (bar scale 100 μm).

Micrographs in **Figure 2** show that surfaces of TGG films were homogeneous although pores were observed on the top of each system, except in the case of FG/Gly film. In addition, bigger and fewer pores were found in the TGG01, TG003, TGG05, TGGO7 and TG009 films, all of them fabricated using the un-milled Ta powder. On the other hand, more

and smaller uniform pores were observed on the surface of the TGG02, TG004, TGG06, TG008 and TGG10 films, in which ball milled Tara powders were introduced. Then, it is clear that this difference could be ascribable to the reduced Tara particles sizes obtained upon ball milling.

Figure 4 presents the AFM surface images of TGG09 and TGG10 films, in which the distribution of Tara powder (non-milled in the case of TGG09 film and milled in the case of TGG10) is observed. AFM surface images do not show great differences in the Tara powder distribution, showing that, in general, Tara powder is well dispersed in the film surface. Only a few agglomerated Tara particles are observed in the surface of the films, as it can be seen in the yellow circles spotted of **Figures 4a** and **4c**.

The effect of the milling ball can be analyzed from two different points of view. First, it seems that the size of the agglomerated particles is slightly higher when non milled Tara is employed, as it can be seen in the agglomeration of Tara particles in **Figures 4a** (TGG09, non-milled Tara) and **4c** (TGG10, milled Tara). Secondly, the size distribution of Tara particles can be observed in the AFM surfaces images presented in **Figures 4b** (TGG09) and **4d** (TGG10). In this case, there is not a very clear difference between the particles size of non-milled (**Figure 4b**) and milled Tara (**Figure 4d**), but it can be detected that milling the Tara powder could reduce the particle size compared to non-milled Tara. In this sense, **Figure 4d** show Tara particles with sizes below 1 μm of diameter, and on the other hand, **Figure 4b** presents, in the bottom-left zone, Tara particles with higher sizes (around 1 μm).

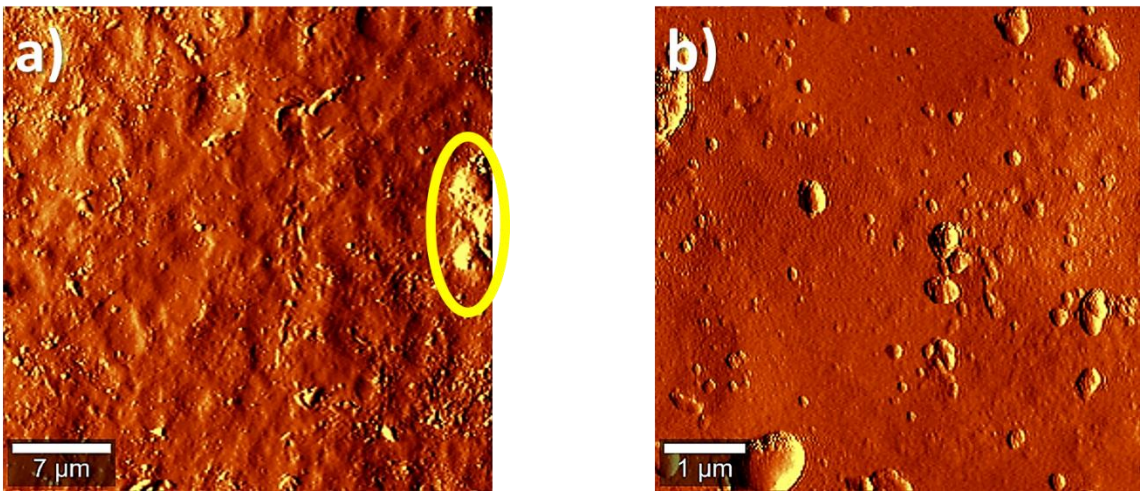

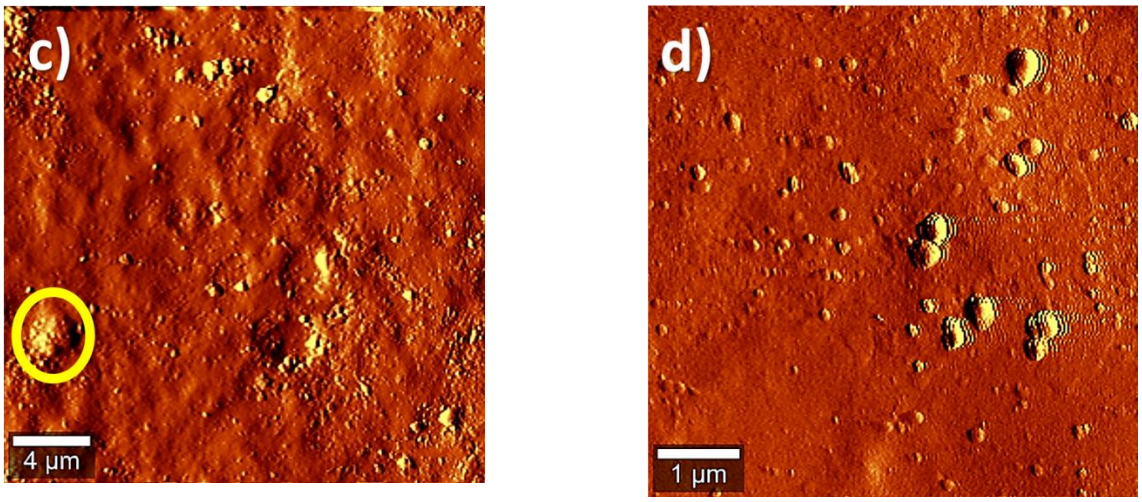

Figure 4. AFM surface images of TGG09 (a and b) and TGG10 (c and d) films.

296

297 **5.5 Thermal stability of films**

298 Preliminary structural and morphological analyses on films TGG01-TGG10 revealed a not
299 negligible effect of Tara granulometry. Films with different structures should manifest
300 different thermal and mechanical behavior. Regarding the thermal stability, it was assessed
301 by TGA analysis. Information about the degradation and mode of decomposition under the
302 effect of heat were also acquired. In **Figure 4**, the TGA thermogram of film TGG02 is
303 presented as an example.

304

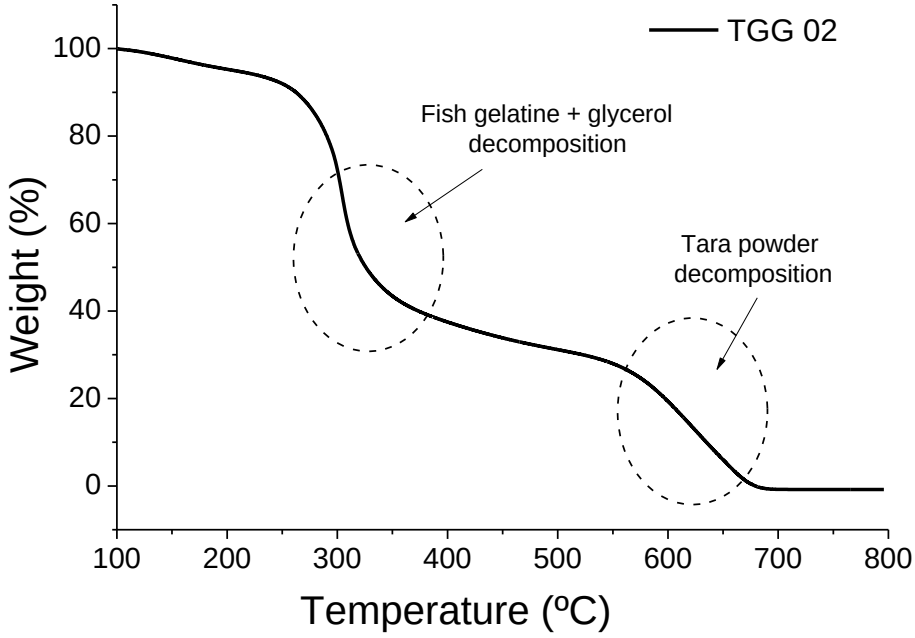

305

306 **Figure 4.** TGA profile of film TGG02.

307

From the thermogram presented in **Figure 4**, two weight losses are clearly detected. Decomposition of fish gelatin-glycerol polymeric structure is detected around 300 ºC, whereas Tara powder degradation begins at 550 ºC. The complete set of thermograms obtained from all the films fabricated are presented in **Figure S6** of the **ESI**.

Additionally, Differential Scanning Calorimetry (DSC) analysis were performed on TGG01-TGG10 films. The DSC measurements were employed for the determination of the glass transition temperature (T_g), measured during the third cycle of the measurement procedure. An example of the glass transition region is presented in **Figure 5**, in which the DSC curve of the TGG02 film is showed, in which the T_g is appears around 62 ºC. The DSC curves obtained from all the films, in which the T_g region is observed, is shown in **Figure S7** of the **ESI**.

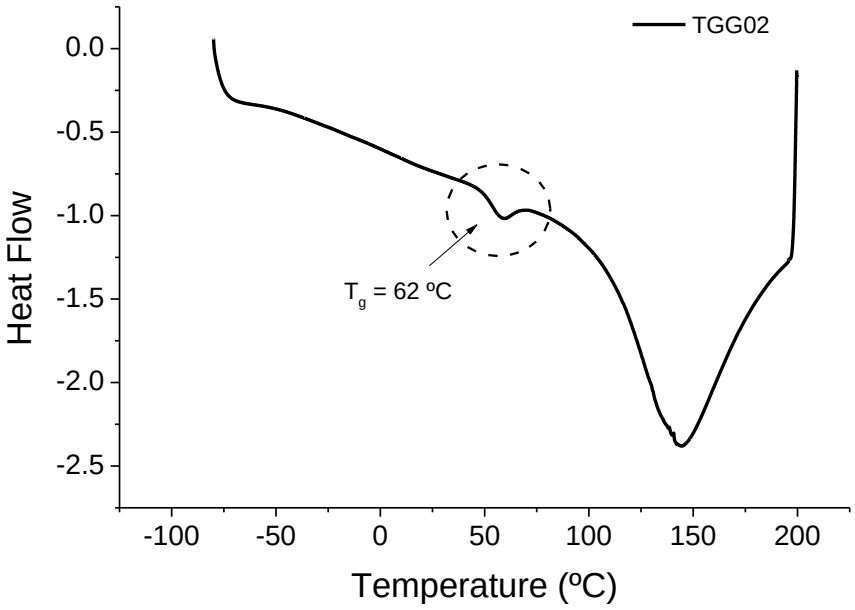

Figure 5. DSC curve (third cycle) obtained for TGG02 film.

All the thermal data derived from TGA and DSC tests corresponding to all the films fabricated are reported in **Table 2**.

Table 2. Thermal properties of all the films prepared. T_g is the glass transition temperature, humidity loss percentage was measured directly as the quantity of mass loss at 100 ºC, $T_{5\%}$ and $T_{10\%}$ are the temperatures at which 5 % and 10 % of mass is lost, and Onset temperature is defined as the temperature at which the decomposition of the material begins.

Film	T_g (°C)	Humidity loss (%)	$T_{5\%}$ (ºC)	$T_{10\%}$ (ºC)	Onset (ºC)

TGG 01	63	9.8	213	245	274
TGG 02	62	6.9	224	268	294
TGG 03	52	10.7	190	218	266
TGG 04	54	10.1	193	237	287
TGG 05	50	10.5	175	207	259
TGG 06	51	7.3	244	261	275
TGG 07	69	9.7	207	244	274
TGG 08	61	8.1	215	251	277
TGG 09	63	6.1	217	263	287
TGG 10	58	5.3	228	268	293
FG/Gly	48	4.1	121	191	264
Ta/Gly	52	11.7	258	269	319

As it can be seen in data in **Table 2**, pure FG films (FG/Gly) present the lower $T_{5\%}$, $T_{10}\%$ and onset temperature values, with temperatures of 121 ºC, 191 ºC and 264 ºC, respectively. Comparing these data with the thermal behavior of pure Tara films (Ta/Gly), values are considerably increased ($T_{5\%}$, $T_{10}\%$ and onset values are 258 ºC, 269 ºC and 319 ºC), indicating that the Tara powder has a better thermal stability that Fish gelatin. In both cases, the quantity of glycerol employed is 20 wt%.

Values of $T_{5\%}$, $T_{10}\%$ and onset temperature in Tara-gelatin films (TGG01 to TGG10) lie between the limit values showed by the FG/Gly and Ta/Gly. In this sense, it is demonstrated the good thermal behavior of composite films respect to pure FG film. This improvement on the thermal behavior depends strongly on the quantity of glycerol, but we can even remark that films with high glycerol content (TGG 05 and TGG 06, with 60 wt% of glycerol) present a good thermal stability (onset temperatures are 259 ºC and 275 ºC).

As expected, the quantity of glycerol has a predominant effect in the thermal stability of the films. In this sense, increasing the glycerol content lowers the $T_{5\%}$ and $T_{10\%}$ temperatures, then affecting negatively to the thermal stability and to the processing or working temperatures. On the other hand, using milled Tara seems to affect positively in the thermal stability of the films. For example, comparing the TGA data of TGG 01 (non-milled Tara) and TGG 02 (milled Tara), it can be seen that $T_{5\%}$, $T_{10\%}$ and onset temperatures are increased up to 20 ºC, indicating that the use of milled Tara also increases the thermal stability of the films, obtaining films stable up to 300 ºC, making them easy processable [31]. Finally, the humidity content values for TGG films vary between the limit values marked for pure Fish gelatin film (4.1 %) and pure Tara film (11.7 %). In this case, the use of milled Tara reduces

the humidity content respect to films with non-milled Tara (compare, for example, humidity content values of TGG 01 and TGG 02 films). This is also a very positive effect in terms of stability and handleability of the films. It is important to remark that similar humidity loss and thermal decomposition profiles were reported by Pulieri *et al.* in the case of Chitosan/gelatin blends [32].

Concerning the analysis of the glass transition temperature, it emerges that TGG films show higher T_g values with respect to FG/Gly, although this difference is not very important (in Ta/Gly film was not possible to measure the T_g temperature precisely). The discussion of the results can be carried out taking into account three different separated effects: (**i**) The influence of the Ta/FG ratio on the T_g, (**ii**) The effect of glycerol weight percentage, and (**iii**), the type of Ta employed (milled or not milled).

Figure 6 shows the T_g variation in all the films as a function of the Ta/FG ratio (**Figure 5a**) and also as a function of glycerol weight percentage (**Figure 5b**).

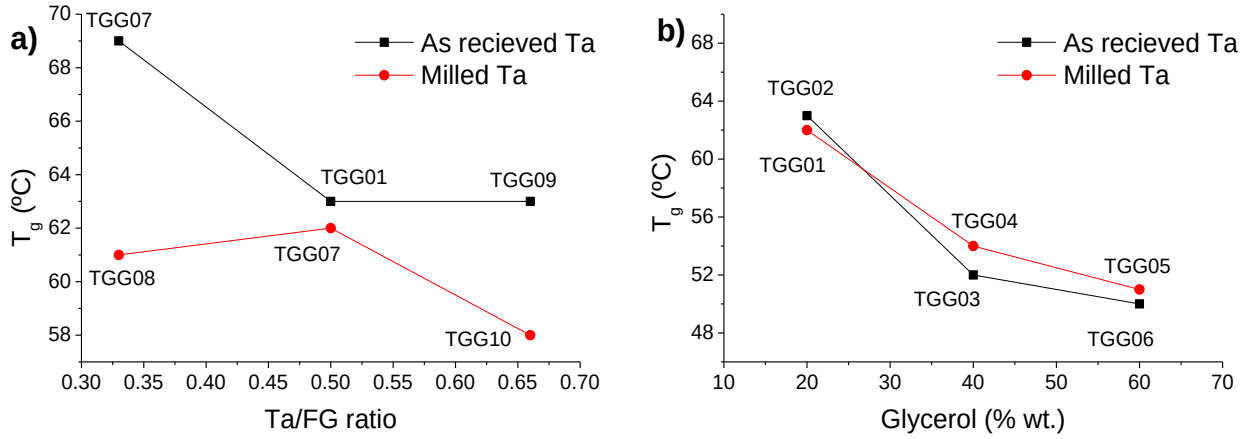

Figure 6. T_g values of films fabricated. a) Films with different Ta/FG ratio; b) Films with different glycerol weight percentage.

Figure 6a shows the influence of the Ta/FG ratio in the glass transition temperature. Having a look at films fabricated using non milled Tara, a reduction of T_g is observed when the Ta/FG ratio increases. On the other hand, the effect of the glycerol weight percentage is clearly observed (**Figure 6b**). As expected, the addition of glycerol decreases the T_g, confirming the role of glycerol as plasticizer. Finally, the third effect is related to the Tara powder employed (non-milled or milled). The analysis of the data in **Figure 6** shows that using milled Tara increases the glass transition temperature, but only when TGG07 vs TGG08 and TGG09 vs TGG10 films are compared (see **Figure 6a**). In these particular cases, T_g is increased around 7 ºC.

5.6 Tensile properties

To analyse the mechanical behaviour of films TGG01-TGG10, tensile properties were measured. Three different parameters were determined from the stress (σ)-strain (ε) curves: Young modulus *E*, stress (σ_{break}, (MPa)) and deformation at break (ε_{break}, (%)). **Figure S8** of the **ESI** shows the stress-strain curves obtained for all the films fabricated, while **Table 3** presents the corresponding mechanical data.

Table 3. Mechanical data of the films TGG01-TGG10.

Film	*E* (MPa)	Δ^1 (MPa)	σ_{break} (MPa)	Δ^1 (MPa)	ε_{break} (%)	Δ^1 (%)
TGG 01	97	13.3	24	2.5	75	7.3
TGG 02	195	18.8	23	1.5	58	6.4
TGG 03	11	2.7	9	2.9	100	11.1
TGG 04	27	5.4	15	3.1	73	9.2
TGG 05	5	1.2	4	0.3	107	8.6
TGG 06	12	4.4	7	2.5	96	14.1
TGG 07	194	19.8	27	3.1	62	13.2
TGG 08	94	21.1	13	2.1	78	4.1
TGG 09	234	17.8	35	5.2	74	17.2
TGG 10	200	21.2	23	1.5	63	12.3
FG/Gly	243	5.9	36	3.8	95	6.1
Ta/Gly	550	31.7	40	13.2	23	7.0

[1]Δ indicate the standard deviation of each value.

Mechanical data presented in **Table 3** indicate that Young's moduli values show a wide variability, from 5 MPa (TGG 05) to 234 MPa (TGG 09), as well as the stress at break, included between 4 MPa (TGG05) and 35 MPa (TGG09). Consequently, the deformation at break range between 23% and 107%.

This variability in the mechanical data can be related to the glycerol content and its plasticization effect, which plays a key role in the mechanical performance of the materials. In order to better highlight this effect, the dependence of the mechanical parameters with the glycerol content is reported in **Figure 7**.

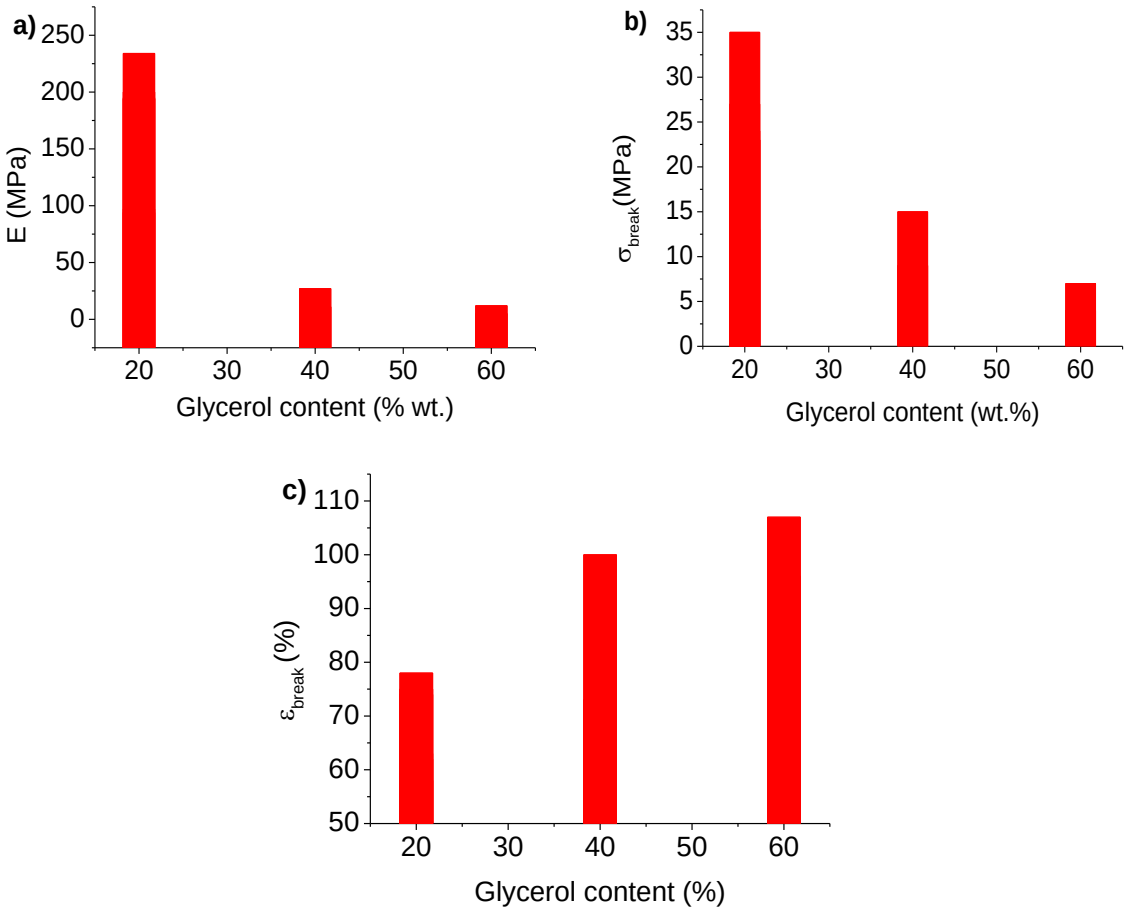

Figure 7. Dependence of the mechanical data of the films with glycerol content. a) Young's moduli, b) Stress at break, and c) Deformation at break.

It can be observed that the Young's moduli, as well as the stress at break decrease when glycerol is added, while the deformation at break increases with the content of glycerol. This behaviour confirms the plasticization effect expected through the addition of glycerol in the initial formulation of the materials.

Having a look at the values individually, TGG09 and TGG10 films present the higher values of Young's moduli (234 and 200 MPa). This is directly related to the Tara powder content, which is higher in these films (2 wt. eq).

In addition to the two main effects discussed above, a not-negligible influence of the Tara grain size on the mechanical properties can be observed. In **Figure 8**, the variation of *E* as function of Ta/FG ratio and type of Tara (milled and not milled) is reported.

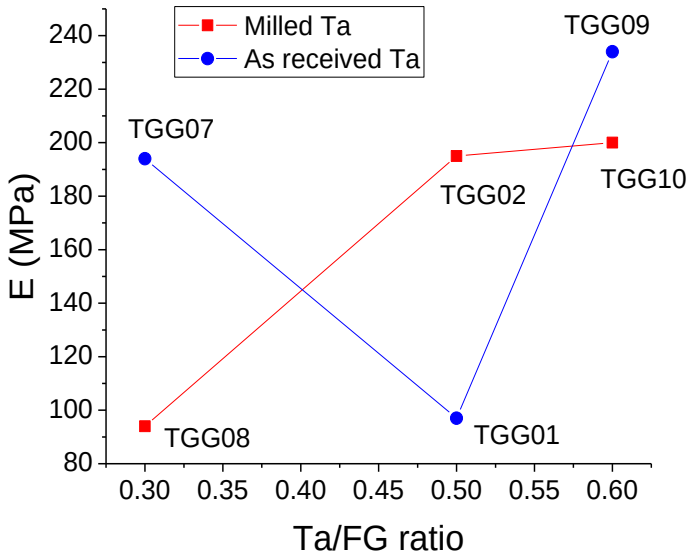

Figure 8. Variation of Young modulus E with the Ta/FG ratio and effect of the ball-milling of Tara gum powder.

From the plots showed in **Figure 8** it is possible to notice a different mechanical behaviour of films containing milled Ta which influences differently the trends of the two series TGG07-TGG01-TGG09 and TGG08-TGG02-TGG10 (**Figure 8**, circled and squared points). Films prepared with not milled Tara show a difference in Young's moduli value of about 100 MPa for Ta/FG ½ ratio (TGG07 vs TGG08) and for Ta/FG ratio of 1/1 (TGG02 vs TGG01), but with opposite trends. In the presence of an excess of Tara, the Young's moduli values are quite similar, with not milled films showing a value slightly higher. Finally, to better compare the curves relative to films containing non-milled and milled Tara, the variation of stress at break and deformation at break of films containing the two different Tara powders is reported in **Figure 9**.

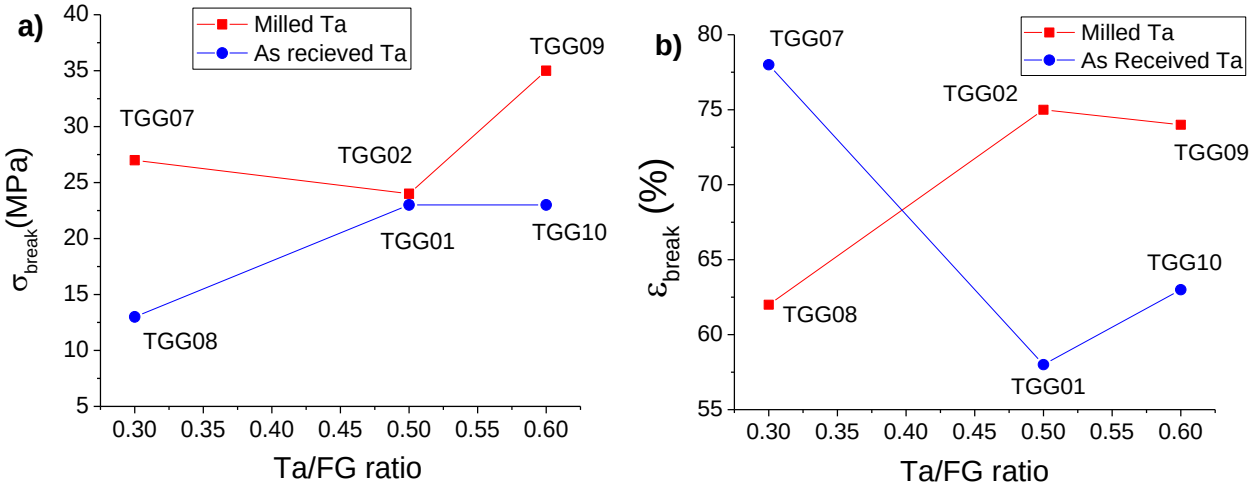

Figure 9. Mechanical data as function of Ta/FG of films containing non-milled or milled Tara gum powder. a) Stress at break; b) Deformation at break.

Data in **Figure 9** indicates that stress at brake is affected by the presence of milled Tara only in films containing with Ta/FG ratio 2/1 or ½, while the mechanical values for Ta/FG ratio of 1/1 are almost coincident (**Figure 9a**). On the contrary, the deformation at brake shows a different behaviour depending of the Tara employed. When non-milled Tara is used, deformation at break grows with the increasing of Tara content, whereas on the other hand when milled Tara is employed the trend is the opposite (**Figure 9b**).

6. Conclusions

Morphological, thermal and mechanical properties of films composed by fish gelatin, Tara gum and glycerol can be tuned by oportune engeneering processes. In particular, by changing the amount of the plasticizer glycerol, it is possible to optimize the composition in terms of thermal behaviour and mechanical properties. Also, the structural effect obtained by the addition of Tara gum resulted relevant. By employing milled Tara instead to the commercial one, it is possible to enhance the thermal stability and improve the mechanical performances of the films. The orign of such effects can be found in a change of the morfology of films prepared with different ingredients, and observed by IR spectroscopy and through SEM and AFM analyses. Influencing the performences of the films by reducing the grain size of the natural gum (Tara in our case) represents a novelty and can lead the way toward further optimization of similar polymers.

Acknowledgments

The financial support provided by FEDER (Fondo Europeo de Desarrollo Regional) and both the Spanish Agencia Estatal de Investigacióon (MAT2017–84501-R) and the Consejería de Educación, Junta de Castilla y León (BU306P18) is gratefully acknowledged.

Data Availability

The raw data required to reproduce these findings cannot be shared at this time due to technical limitations.

References

[1] R. Rodríguez-Rodríguez, H. Espinosa-Andrews, C. Velasquillo-Martínez, Z. Y. García-Carvajal, Composite hydrogels based on gelatin, chitosan and polyvinyl alcohol to biomedical applications: a review, Int. J. Polym. Mater. 69 (2015) 1-20. https://doi.org/10.1080/00914037.2019.1581780.
[2] T. Huang, Z. Fang, H. Zhao, D. Xu, W. Yang, W. Yu, J. Zhang, Physical properties and release kinetics of electron beam irradiated fish gelatin films with antioxidants of bamboo leaves, Food Bioscience, 36 (2020), 100597. https://doi.org/10.1016/j.fbio.2020.100597.
[3] T. Huang, J. Lin, Z. Fang, W. Yu, Z. Li, D. Xu, W. Yang, J. Zhang, Food and Bioprocess Technology, 13 (2020), 522-532. https://doi.org/10.1007/s11947-020-02409-w.
[4] P. Díaz-Calderón, L. Caballero, F. Melo, J. Enrione, Molecular configuration of gelatin–water suspensions at low concentration, Food Hydrocoll. 39 (2014) 171-79. https://doi.org/10.1016/j.foodhyd.2013.12.019.
[5] Q. Xing, K. Yates, C. Vogt, Z. Qian, M.C. Frost, F. Zhao, Increasing mechanical strength of gelatin hydrogels by divalent metal ion removal, Sci. Rep. 4 (2014) 1-10. https://doi.org/10.1038/srep04706.
[6] H. Massoumi, J. Nourmohammadi, M.S. Marvi, F. Moztarzadeh, Comparative study of the properties of sericin-gelatin nanofibrous wound dressing containing halloysite nanotubes loaded with zinc and copper ions, Int. J. Polym. Mater. Polym. Biomater. 68 (2019) 1-12. https://doi.org/10.1080/00914037.2018.1534115.
[7] W.W. Thein-Han, J. Saikhun, C. Pholpramoo, R.D.K. Misra, Y. Kitiyanant, Chitosan–gelatin scaffolds for tissue engineering: Physico-chemical properties and biological response of buffalo embryonic stem cells and transfectant of GFP–buffalo embryonic stem cells. Acta Biomater. 5 (2009) 3453-3466. https://doi.org/10.1016/j.actbio.2009.05.012.
[8] X. Feng, V. K. Ng, M. Mikš-Krajnik, H. Yang, Effects of Fish Gelatin and Tea Polyphenol Coating on the Spoilage and Degradation of Myofibril in Fish Fillet During Cold Storage, Food and Bioprocess Technology, 10 (2017), 89-102. https://doi.org/10.1007/s11947-016-1798-7.
[9] J. Rose, S. Pacelli, A. Haj, H. Dua, A. Hopkinson, L. White, F. Rose, Gelatin-based materials in ocular tissue engineering, Materials 7 (2014) 7, 3106-3135. https://doi.org/10.3390/ma7043106.
[10] J.R. Dias, S. Baptista-Silva, C.M. Oliveira, A. de Sousa, A.L. Oliveira, P.J. Bartolo, P.L. Granja, In-situ crosslinked electrospun gelatin nanofibers for skin regeneration, Eur. Polym. J. 95 (2017) 161-173. https://doi.org/10.1016/j.eurpolymj.2017.08.015.
[11] M. S. Rahman, G. S. Al-Saidi, N. Guizani, Thermal characterisation of gelatin extracted from yellowfin tuna skin and commercial mammalian gelatin, Food Chemistry 108 (2008) 472-481. https://doi.org/10.1016/j.foodchem.2007.10.079.
[12] A. Duconseille, T. Astruc, N. Quintana, F. Meersman, V. Sante-Lhoutellier, Gelatin structure and composition linked to hard capsule dissolution: A review, Food Hydrocoll. 43 (2015) 360-376. https://doi.org/10.1016/ j.foodhyd.2014.06.006.

[13] E. Jeevithan, Z. Qingbo, B. Bao, W. Wu, Biomedical and Pharmaceutical Application of Fish Collagen and Gelatin: A Review, Journal of Nutritional Therapeutics, 2 (2013), 218-227.
[14] A. Etxabide, I. Leceta, S. Cabezudo, P. Guerrero, K. de la Caba, Sustainable fish gelatin films: From food processing waste to compost, ACS Sustainable Chem. Eng. 4 (2016) 4626-4634. https://doi.org/10.1021/acssuschemeng.6b00750.
[15] A. Mannu, S. Garroni, J. Ibanez Porras, A. Mele, Available technologies and materials for waste cooking oil recycling, Processes 8 (2020) 366. https://doi.org/10.3390/pr8030366.
[16] M. Bocqué, C. Voirin, V. Lapinte, S. Caillol, J.J. Robin, Petrobased and bio-based plasticizers: Chemical structures to plasticizing properties. J. Polym. Sci., Part A: Polym. Chem. 54 (2016) 11-33. https://doi.org/10.1002/pola.27917.
[17] A.A. Karim, R. Bhat, Fish gelatin: properties, challenges, and prospects as an alternative to mammalian gelatins, Food Hydrocoll. 23 (2009) 563-579. https://doi.org/10.1016/j.foodhyd.2008.07.002.
[18] M. Ramos, A. Valdés, A. Beltrán, M.C. Garrigós, Gelatin-based films and coatings for food packaging applications, Coatings 6 (2016) 41. https://doi.org/10.3390/coatings6040041.
[19] P.K. Binsi, N. Nayak, P.C. Sarkar, C.G. Joshy, G. Ninan, C.N. Ravishankar, Gelation and thermal characteristics of microwave extracted fish gelatin-natural gum composite gels, J. Food Sci. Technol. 54 (2017) 518-530. https://doi.org/10.1007/s13197-017-2496-9.
[20] Y. Wu, W. Ding, L. Jia, Q. He, The rheological properties of tara gum (Caesalpinia spinosa), Food Chemistry 168 (2015) 366-371. https://doi.org/10.1016/j.foodchem.2014.07.083.
[21] A. Mortensen, F. Aguilar, R. Crebelli, A. Di Domenico, M. J. Frutos, P. Galtier, D. Gott, U. Gundert-Remy, C. Lambré, J.-C. Leblanc, O. Lindtner, P. Moldeus, P. Mosesso, A. Oskarsson, D. Parent-Massin, I. Stankovic, I. Waalkens-Berendsen, R. A. Woutersen, M. Wright, M. Younes, L. Brimer, A. Christodoulidou, F. Lodi, A. Tard, B. Dusemund, Re-evaluation of tara gum (E 417) as a food additive, EFSA Journal, 15, 6 (2017), e04863. https://doi.org/10.2903/j.efsa.2017.4863.
[22] Available online at: http://www.lapigelatine.com/wp-content/uploads/2017/01/fish.gelatine.edible.grade_.pdf (accessed on 10/10/2020).
[23] J. Chong, O. Soufan, C. Li, I. Caraus, S. Li, G. Bourque, D.S. Wishart, J. Xia, MetaboAnalyst 4.0: towards more transparent and integrative metabolomics analysis, Nucl. Acids Res. 46 (2018) 486-494. https://doi.org/10.1093/nar/gky310.
[24] F. Delogu, G. Gorrasi, A. Sorrentino. Fabrication of polymer nanocomposites via ball milling: Present status and future perspectives, Prog. Mater. Sci. 86 (2017) 75-126. https://doi.org/10.1016/j.pmatsci.2017.01.003.
[25] B. S. Pascual, M. Trigo-López, J. A. Reglero Ruiz, J. L. Pablos, J. C. Bertolín, C. Represa, J. V. Cuevas, Félix C. García, J. M. García, Porous aromatic polyamides the easy and green way, European Polymer Journal, 116 (2019), 91-98. https://doi.org/10.1016/j.eurpolymj.2019.03.058.

[26] S. Basu, U.S. Shivhare, T.V. Singh, V.S. Beniwal, Rheological, texture and spectral characteristics of sorbitol substituted mango jam, J. Food Eng. 105 (2011) 503-512. https://doi.org/10.1016/j.jfoodeng.2011.03.014.
[27] UNE-EN 13432:2001 Requirements for packaging recoverable through composting and biodegradation. Test scheme and evaluation criteria for the final acceptance of packaging. 2001.
[28] J. M. Chalmers, N. J. Everall, Polymer Analysis and Characterization by FTIR, FTIR-Microscopy, Raman Spectroscopy and Chemometrics, Int. J. Polym. Anal. Characf. 5 (1999), 223-245. https://doi.org/10.1080/10236669908009739.
[29] M. S. Lindblad, B. M. Keyes, L. M. Gedvilas, T. G. Rials, S. S. Kelley, FTIR imaging coupled with multivariate analysis for study of initial diffusion of different solvents in cellulose acetate butyrate films, Cellulose, 15 (2008), 23-33. Http://doi.org/10.1007/s10570-007-9173-5.
[30] B. Worley, R. Powers, Multivariate analysis in metabolomics, Curr. Metabolomics 1 (2013) 92-107. https://doi.org/10.2174/2213235X11301010092.
[31] M.A. Meador, Recent advances in the development of processable high-temperature polymers. Annu. Rev. Mater. Sci. 28 (1998) 599-630. https://doi.org/10.1146/annurev.matsci.28.1.599.
[32] E. Pulieri, V. Chiono, G. Ciardelli, G. Vozzi, A. Ahluwalia, C. Domenici, F. Vozzi, P. Giusti, Chitosan/gelatin blends for biomedical applications, J. Biomed. Mater. Res. A. 86 (2008) 311-322. https://doi.org/10.1002/jbm.a.31492.